

压气机动态模型的建立及喘振过程分析

王伟才, 王银燕

(哈尔滨工程大学动力与能源工程学院, 黑龙江 哈尔滨 150001)

摘 要: 在 SIMULINK 环境中, 建立了压气机动态数学模型。为了模拟压气机喘振和旋转失速现象, 压气机特性图被延伸到负流量区域, 还考虑到了气体通过压气机的延迟。模拟了压气机的喘振过程, 并对压气机压力信号进行 FFT 变换, 检测了压气机喘振。仿真结果表明: 模型能预测压气机喘振过程中压力、流量和转速的振荡频率和振幅; 压缩系统的转动惯量、稳压室容积等结构参数影响喘振特性; 模型动态调节特性好, 可用于压气机控制系统模型, 具有广泛实用性。

关 键 词: 压气机; 动态模型; 喘振; FFT

中图分类号: TK423. 5 文献标识码: A

引 言

压气机被广泛使用在不同的领域, 如燃气轮机、增压柴油机、增压锅炉等。旋转式的轴流压气机和离心压气机的稳定工作区域受其内部气体流动限制, 如高流量区的阻塞、低流量区喘振和旋转失速。压气机喘振和旋转失速这样的非稳态特性不仅引起压气机性能下降, 而且造成叶片及旋转轴的剧烈振动, 从而可能导致压气机叶片损坏, 甚至压气机停止工作。因此, 预测喘振和旋转失速这种非稳定特性非常重要。

Moore 和 Greitzer 在 1986 年建立了著名的旋转失速和压气机喘振的统一模型(MG 模型)^[1], 提出了采用系统工作的 B 参数来判断压气机失稳模式。1992 年 Fink 提出了离心压气机非定转速喘振模型^[2]。随后 J. T. Gravidahl 和 F. Willems 等人对压气机喘振模型和喘振控制进行了研究^[3~7]。王云辉等人还将 MG 模型扩展到了湿压缩系统中^[8]。

本文建立了离心压气机系统动态模型。为了检测喘振, 对压力信号进行了快速傅立叶变换和谐波分析。计算分析表明: 该动态模型实时性和调节特性好, 可以作为压气机喘振控制系统仿真模型。

1 仿真模型

压气机及其动态等效系统如图 1 所示。系统包括: 压气机、进口和出口管道、稳压室、阀门以及驱动电机。将压气机通道视为等效长的管道, 压气机动叶轮等效于一个促动盘。气体经过促动盘后, 压力升高。压气机增压比通过压气机特性图来求得。通常, 通过试验只能得到压气机喘振线右侧的特性图, 为了计算压气机喘振区域的压比, 采用多项式拟合的方法扩展压气机特性。

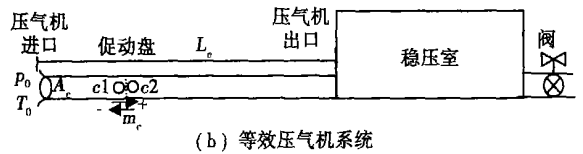
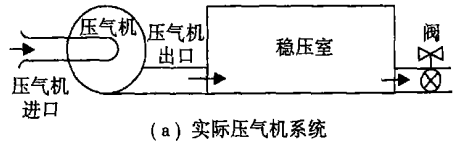


图 1 压气机系统简图

以离心压气机为研究对象, 采用三次方程来拟合喘振线左边到零流量区域的压力曲线:

$$\pi_c = \pi_{c0} + H \left[1 + \frac{3}{2} \left(\frac{m_c}{W} - 1 \right) - \frac{1}{2} \left(\frac{m_c}{W} - 1 \right)^2 \right]^3 \quad (1)$$

式中: π_c —增压比, π_{c0} —零流量时的增压比; m_c —压气机质量流量, W 、 H 的值如图 2 所示。

采用二次方程来拟合负流量区域的压力曲线:

$$\pi_c = \pi_{c0} + H m_c / 2 W^2 \quad (2)$$

压气机零流量时的压比依据守恒方程求出:

$$\pi_{c0} = \left[1 + \frac{k-1}{2kRT_{c1}} \omega_c^2 (r_{c2}^2 - r_{c1}^2) \right]^{\frac{k}{k-1}} \quad (3)$$

式中: k —气体比热比; R —为气体常数; ω_c —压气机角速度; r_{c1} —压气机叶轮进口平均半径; r_{c2} —压气机叶轮出口外半径。

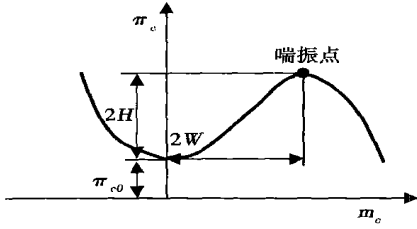


图 2 压气机特性扩展图

压气机的流量可由下式求得:

$$\frac{dm_c}{dt} = \frac{p_{c2} - p_m}{L_c / A_c} \quad (4)$$

式中: p_m —稳压室的压力; L_c / A_c —等效管道的长度与横截面积之比:

$$\frac{L_c}{A_c} = \int_{\text{压气机及进出口管道}} \frac{dl}{A(l)} \quad (5)$$

考虑到压气机动态效果, 采用一阶瞬态响应模型来模拟压气机的响应:

$$\frac{d\pi_c}{dt} = \frac{1}{\tau} (\pi_{c_{ss}} - \pi_c) \quad (6)$$

式中: $\pi_{c_{ss}}$ —压气机增压比的稳态值; τ —时间延迟, 可由试验或经验公式确定。

压气机转速可由角动量守恒方程求得:

$$\frac{dn_c}{dt} = \frac{30}{\pi I_c} (M_t - M_c) \quad (7)$$

式中: I_c —压气机转动惯量; M_t —电机驱动的扭矩。

压气机的扭矩可由能量方程求得:

$$M_c = \frac{30kRm_c T_{c1}}{\pi n_c (k-1) \eta_c} (\pi_c^{(k-1)/k} - 1) \quad (8)$$

式中: T_{c1} —压气机进口温度; η_c —压气机效率。扭矩可直接由压气机无量纲流量 ϕ_c 和扭矩 Γ_c 之间的线性关系求得:

$$\Gamma_c = c_1 \phi_c + c_2 \quad (9)$$

式中: c_1, c_2 —常数, 可根据压气机正流量区域的试验数据拟合得到。

稳压室模型采用充满与排空法, 其能量守恒方程为:

$$\frac{d(u_m m_m)}{dt} = h_{m_i} \frac{dm_{m_i}}{dt} - h_{m_o} \frac{dm_{m_o}}{dt} \quad (10)$$

式中: u_m —稳压室内气体比内能; m_m —稳压室内气体质量; h_{m_i} —稳压室进口气体比焓; m_{m_i} —稳压室进口气体质量; h_{m_o} —稳压室出口气体比焓; m_{m_o} —稳

压室出口气体质量。

将式(10)展开, 并整理可以求得稳压室温度的变化率:

$$\frac{dT_m}{dt} = \frac{1}{m_m} \left[kT_{m_i} \frac{dm_{m_i}}{dt} - kT_{m_o} \frac{dm_{m_o}}{dt} - T_m \frac{dm_m}{dt} \right] \quad (11)$$

稳压室内气体压力, 可由状态方程求得:

$$p_m = m_m R T_m / V_m \quad (12)$$

阀的流量可由公式 $m_t = k_t \sqrt{p_m - p_0}$ 求得, 其中 k_t 为阀的增益。

在 Matlab/SIMULINK 环境中, 搭建的压气机动态系统仿真模型如图 3 所示。

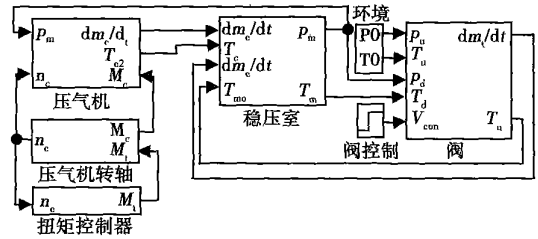


图 3 压气机系统的 SIMULINK 程序

为了实时检测压气机喘振, 采用快速离散傅立叶变换(FFT)频域方法来检测喘振频率信号。FFT 的时间抽样算法具体步骤为:

设 $x(n)$ 是一个长度为 N 的有限长序列, 定义 $x(n)$ 的 N 点离散傅立叶变换(DFT)为:

$$X(k) = \sum_{n=0}^{N-1} x(n) e^{-j\frac{2\pi}{N}kn}, k=0, 1, \dots, N-1 \quad (13)$$

定义 $e^{-j\frac{2\pi}{N}kn} = W_N^{kn}$, 利用 $W_N^{kn} = W_N^{k(n+N)} = W_N^{(k+N)n}$ 和 $W_N^{kN+N/2} = -W_N^{kn}$, 将 N 点的 DFT 转换为 $N/2$ 点的 DFT, 当 $N=2^r$ 时, 将 $x(n)$ 按奇偶分成 $N/2$ 的序列:

$$x_1(r) = x(2r), 0 \leq r \leq N/2-1 \quad (14)$$

$$x_2(r) = x(2r+1), 0 \leq r \leq N/2-1 \quad (15)$$

则:

$$X(k) = \sum_{n=0}^{N-1} x(n) W_N^{kn} = \sum_{r=0}^{N/2-1} x(2r) W_N^{k2r} + \sum_{r=0}^{N/2-1} x(2r+1) W_N^{k(2r+1)} = X_1(k) + W_N^k X_2(k), k=0, 1, \dots, N-1 \quad (16)$$

式中: $X_1(k) = \sum_{r=0}^{N/2-1} x_1(r) W_{N/2}^{kr} = \text{DFT}[x_1(r)]$

$X_2(k) = \sum_{r=0}^{N/2-1} x_2(r) W_{N/2}^{kr} = \text{DFT}[x_2(r)]$

由于 $X_1(k)$ 和 $X_2(k)$ 都是 $N/2$ 点的 DFT, 且 $W_N^{kN/2} = -W_N^{kn}$, 所以 $X(k)$ 也可以表示为:

$$X(k) = X_1(k) + W_N^k X_2(k), k = 0, 1, \dots, N/2 - 1 \quad (17)$$

$$X(k + N/2) = X_1(k) - W_N^k X_2(k), k = 0, 1, \dots, N/2 - 1 \quad (18)$$

这就将 N 点的 DFT 分解为两个 $N/2$ 点的 DFT 的运算。 $N/2$ 点的 DFT 还可以再分解为 $N/4$ 点 DFT, 共可以分解为 r 级, 最后达到 $N/2$ 个 2 点 DFT 运算。

对压力信号进行 FFT 变换, 求出信号的频谱谱, 再进行谐波分析求出各次谐波的频率和幅值, 并由下式求出总的谐波失真度 (THD):

$$\%THD = \frac{100 \sqrt{A(f_2)^2 + A(f_3)^2 + \dots + A(f_m)^2}}{A(f_1)} \quad (19)$$

式中: $A(f_1)$ —基波的幅值; $A(f_m)$ —第 m 次谐波的幅值, m —总的谐波次数。

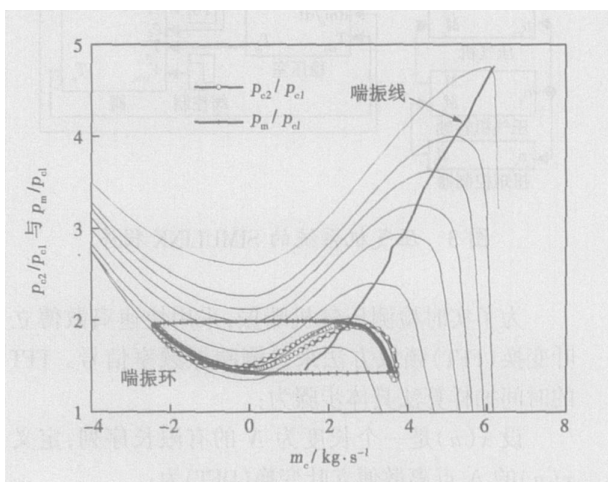


图 4 稳压室容积 0.5 m^3 时的喘振环

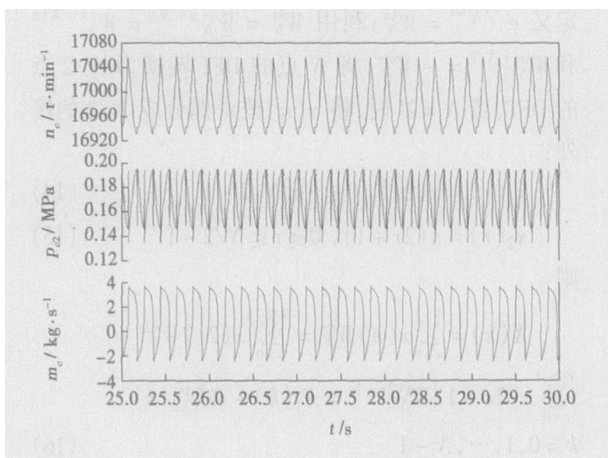


图 5 稳压室容积 0.5 m^3 时的压气机参数变化曲线

2 仿真结果与分析

为了分析压气机喘振问题, 对不同结构参数的压气机动态性能进行了仿真。压气机特性图为试验

曲线, 并扩展了其喘振线左边的压力曲线。本文压气机动态模型的仿真步长为 0.0001 s , 其求解器采用 ode5 (Dormand—Prince) 方法, 仿真时间 30 s , 相应的信号采样频率为 10 kHz , 驱动压气机的扭矩为 $100 \text{ N} \cdot \text{m}$, 稳压室的容积为 0.5 m^3 , 环境压力为 0.1 MPa , 环境温度为 300 K , 稳压室初试条件为 0.1 MPa 、 300 K 。通过仿真实验, 将阀门开度逐渐关小, 使得压气机运行点越过喘振线, 进入喘振区域。阀门开度为 10% 的仿真结果如图 4~图 6 所示。

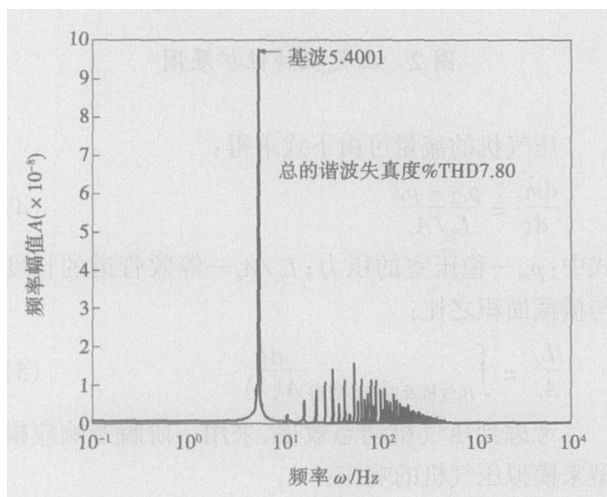


图 6 稳压室容积 0.5 m^3 时的压气机喘振频谱

由压气机特性曲线图 4 可以明显看出喘振环, 由其参数变化曲线图 5 可以看出压气机的转速、出口压力和流量都发生波动, 其振幅分别为 125 r/min 、 0.0605 MPa 和 6.14 kg/s 。并对压气机出口压力信号进行 FFT 变换以及谐波分析, 结果如图 6 所示, 求得喘振频率为 5.4 Hz , 总的谐波失真度 $\%THD$ 为 7.80 。压气机喘振的振幅和频率都不随时间而发生变化。

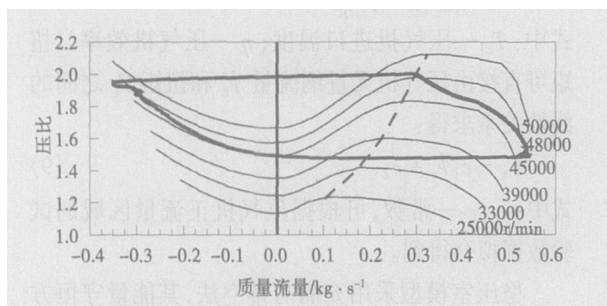


图 7 稳压室与环境之间的压比和压气机质量流量在压气机特性图上的轨迹^[6]

为了检验仿真模型的正确性, 参考了文献[6]的运行数据, 如图 7 所示, 该图中的喘振环与图 4 中

p_m/p_{c1} 的喘振环的趋势基本一致,由于两压气机大小不一样,因此在喘振环的大小上略有差异。这表明本文仿真模型基本正确,可以用来预测压气机喘振过程,避免压气机喘振试验带来的破坏机组部件。

为了研究稳压室容积和压气机转动惯量对喘振的影响,进行了动态仿真:

(1) 当稳压室容积增加到 1 m^3 时,其仿真结果如图 8~图 10 所示。由压气机运行轨迹图 8 可以看出容积增大后仍有喘振环,由其参数变化曲线图 9 可以看出压气机的转速、出口压力和流量同样都发生波动,其振幅分别为 220 r/min 、 0.058 2 MPa 和 6.10 kg/s ;与稳压室容积为 0.5 m^3 相比,转速振幅增加了 76%,压力和流量振幅几乎相等。对压气机出口压力信号进行 FFT 变换以及谐波分析,如图 10 所示,喘振频率为 3.0 Hz ,总的谐波失真度 %THD 为 34.84。相比稳压室为容积 0.5 m^3 时,其频率降低了 2.4 Hz ,相应的周期延长。压气机喘振的振幅和频率同样都不随时间而变化。

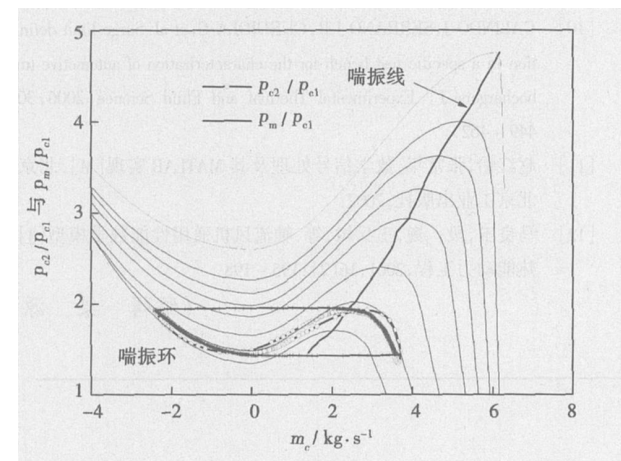


图 8 稳压室容积 1 m^3 时的喘振环

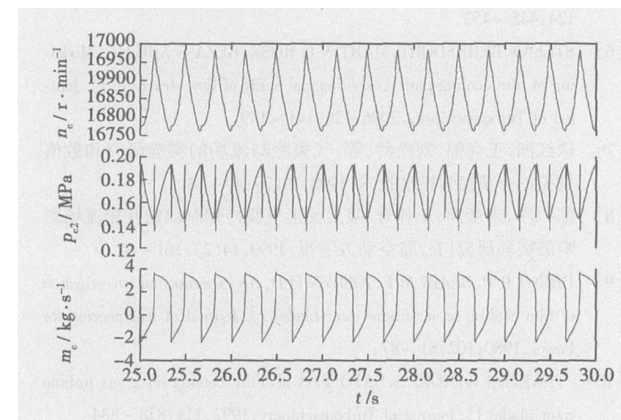


图 9 稳压室容积 1 m^3 时的压气机参数变化曲线

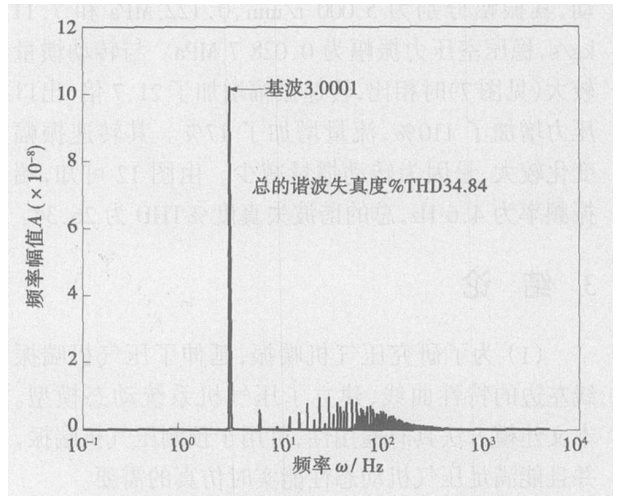


图 10 稳压室容积 1 m^3 时的压气机喘振频谱

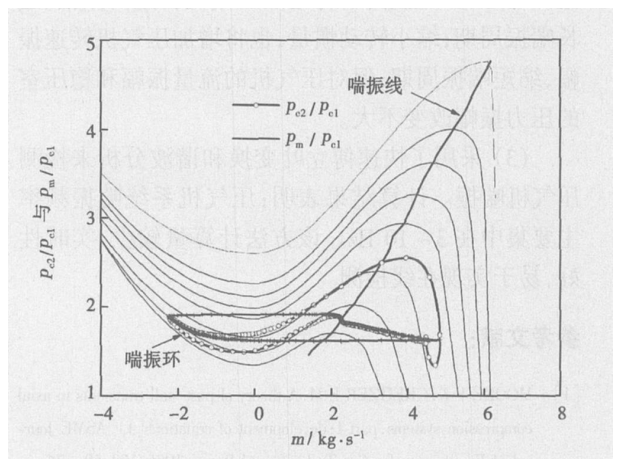


图 11 转动惯量缩小到 2% 时的压气机参数变化曲线

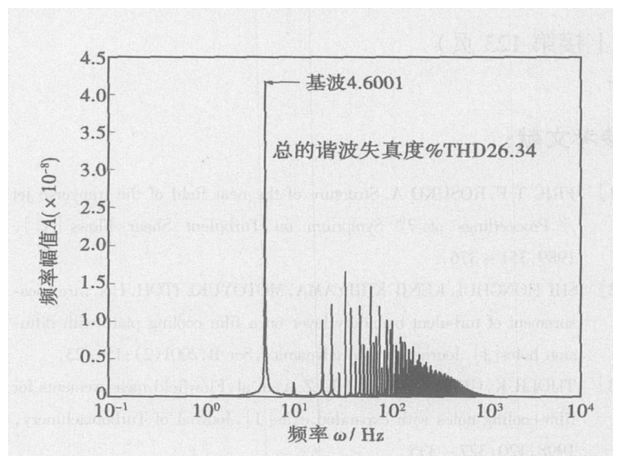


图 12 转动惯量缩小到 2% 时的压气机喘振频谱

(2) 当稳压室容积增加到 1 m^3 和转动惯量缩小到 2% 时,其仿真结果如图 11 和图 12 所示。由图 11 可知,压气机的转速、出口压力和流量均发生波

动,其振幅分别为 5 000 r/min、0.122 MPa 和 7.11 kg/s,稳压室压力振幅为 0.028 7 MPa。与转动惯量较大(见图 7)时相比,转速振幅增加了 21.7 倍,出口压力增加了 110%,流量增加了 17%。其转速振幅变化较大,是因为转动惯量减少。由图 12 可知,喘振频率为 4.6 Hz,总的谐波失真度%THD 为 26.34。

3 结 论

(1) 为了研究压气机喘振,延伸了压气机喘振线左边的特性曲线,建立了压气机系统动态模型。本文建模方法具有通用性,可用于预测压气机喘振,并且能满足压气机动态性能实时仿真的需要。

(2) 压气机喘振由实际系统的结构形状来决定。增加稳压室容积,将增加压气机转速的振幅、延长喘振周期;缩小转动惯量,也将增加压气机转速振幅,缩短喘振周期;但对压气机的流量振幅和稳压室的压力振幅改变不大。

(3) 采用了快速傅立叶变换和谐波分析来检测压气机喘振。计算结果表明:压气机系统喘振频率主要集中在 3~10 Hz。该方法计算量较少、实时性好,易于实现在线检测。

参考文献:

[1] MOORE F K, GREITZER E M. A theory of post-stall transients in axial compression systems. part I: development of equations[J]. ASME Journal of Engineering for Gas Turbines and Power, 1986, 108: 68-76.

[2] FINK D A, CUMSTY N A, GREITZER E M. Surge dynamics in a free-spool centrifugal compressor system[J]. ASME Journal of Turbomachinery, 1992, 114: 321-332.

[3] JAN TOMMY GRAVDAHL. Modeling and control of surge and rotating stall in compressors[D]. Norway; Norwegian University of Science and Technology, 1998.

[4] FRANCISCUS P T WILLEMS. Modeling and bounded feedback stabilization of centrifugal compressor surge[D]. Eindhoven; Technische Universiteit Eindhoven, 2000.

[5] CORINA H J MEULEMAN. Measurement and unsteady flow modelling of centrifugal compressor surge[D]. Eindhoven; Technische Universiteit Eindhoven, 2002.

[6] THEOTOKATOS G, KYRIATOS N P. Diesel engine transient operation with turbocharger compressor surging[R]. 2001 Sae World Congress, 2001-01-1241.

[7] SCHMITZ M B, FITZKY G. Surge cycle of turbochargers; simulation and comparison to experiment[s]. Proceedings of ASME Turbo Expo 2004, GT2004-53036.

[8] 王云辉, 刘敏, 孙聿峰, 等. 湿压缩对压缩系统失速后瞬态响应得影响分析[J]. 热能动力工程, 2003, 18(1): 67-70.

[9] HEYWOOD J B. Internal combustion engine fundamentals[M]. New York: McGraw-Hill Book Company, 1988.

[10] GALINDO J, SERRANO J R, GURDIOLA C, et al. Surge limit definition in a specific test bench for the characterization of automotive turbochargers[J]. Experimental Thermal and Fluid Science 2006 30: 449-462.

[11] 赵红怡, 张常年. 数学信号处理及其 MATLAB 实现[M]. 北京: 北京工业出版社, 2002.

[12] 马良玉, 段巍, 王兵树, 等. 轴流风机通用性能数学模型[J]. 热能动力工程, 2001, 16(2): 195-198.

(编辑 渠源)

(上接第 123 页)

参考文献:

[1] FRIC T F, ROSHKO A. Structure of the near field of the transverse jet //Proceedings of 7th Symposium on Turbulent Shear Flows [C]. 1989. 351-376.

[2] SHI HONGHUI, KENJI KIRIYAMA, MOTOYUKI ITOH. Hot wire measurement of turbulent boundary layer on a film cooling plate with diffusion holes[J]. Journal of Hydrodynamics, Ser B, 2001(2): 15-23.

[3] THOLR K, GRITSCH M, SCHULZ A, et al. Flowfield measurements for film-cooling holes with expanded exits[J]. Journal of Turbomachinery, 1998, 120: 327-335.

[4] AJERSCH P, ZHOU J M, KETTLERS, et al. Multiple jets in a crossflow [J]. Detailed Measurements and Numerical Simulations, 1997, 119: 331-342.

[5] MARC D FOIANKA, CUTBIRTH J MMICHAEL, BOGARD DAVID

G. Three component velocity field measurements in the stagnation region of a film cooled turbine vane[J]. Journal of Turbomachinery, 2002, 124: 445-452.

[6] STEFAN BERNSDORT, MARTIN G ROSE, REZA S ABHARI. Modeling of film cooling- part I: experimental study of flow structure[J]. Journal of Turbomachinery, 2006, 128: 141-149.

[7] 徐红洲, 王尚锦, 刘松龄, 等. 气膜冷却流场的实验研究和数值模拟的分析[J]. 推进技术, 1998, 19(2): 47-53.

[8] 陈浮, 宋彦萍, 王仲奇. 吸力面上气膜冷却对涡轮叶栅流场影响的实验研究[J]. 航空动力学报, 1999, 14(2): 161-65.

[9] DRING R P, BLAIRM F, JOSLYN H D. An experimental investigation of film cooling on a turbine rotor blade[J]. Journal of Engineering for Power, 1980, 102: 81-87.

[10] TAKEISHI K, AOKI S, SATO T, et al. Film cooling on a gas turbine rotor blade[J]. Journal of Turbomachinery, 1992, 114: 828-834.

(编辑 渠源)

低温热能发电的研究现状和发展趋势 = **The Latest Research Findings Concerning Low-temperature Heat Energy-based Power Generation and its Development Trend** [刊, 汉] / GU Wei, WENG Yi-wu, WENG Shi-lie (College of Mechanical and Power Engineering under Shanghai Jiaotong University, Shanghai, China, Post Code: 200030), CAO Guang-yi (College of Electronic Information under Shanghai Jiaotong University, Shanghai, China, Post Code: 200030) // Journal of Engineering for Thermal Energy & Power. — 2007, 22(2). — 115 ~ 119

The utilization of low-temperature heat energy is of major significance because of its rich variety and huge quantity available worldwide. The current research results of low-temperature heat-energy power-generation technology are described along with its development trend. The above-mentioned technology is mainly used for solar-energy cogeneration systems, industrial waste heat-based power generation, geothermal power generation as well as power generation by utilizing biomass energy and ocean temperature difference etc. Nowadays, the research on low-temperature heat energy power generation has been mainly focused on working medium thermophysical properties, environmental protection performance and cycle optimization. The effective methods employed to raise the low-temperature and high-temperature heat energy power-generation efficiency involve research on the following cycles: hybrid working medium cycle, Kalina cycle, recuperative and ammonia-absorption type refrigeration cycle. In addition to the above, system optimized control based on finite time thermodynamics etc. was also studied. **Key words:** low-temperature heat energy, organic matter Rankine cycle, thermal power generation

旋转对气冷涡轮内部流场影响的PIV测量 = **PIV Measurements of the Impact of Rotation on the Flow Fields in a Gas-cooled Turbine** [刊, 汉] / YUAN Feng, ZHU Xiao-cheng, DU Zhao-hui (College of Mechanical and Power Engineering under Shanghai Jiaotong University, Shanghai, China, Post Code: 200030) // Journal of Engineering for Thermal Energy & Power. — 2007, 22(2). — 120 ~ 123, 128

Experimental measurements have been performed of the flow fields in an air-cooled turbine by using PIV (Particle Image Velocimeter) speed measurement technology under both rotating and non-rotating conditions to study the impact of rotation on the flow fields in the air-cooled turbine. In the meantime, the impact of different jet-flow air blowing ratios on the flow fields in the turbine was also studied by changing the air blowing ratio ($M=1.5, 2$). The test results show that there exists an evident wake zone near the downstream of the cooling hole jet-flow. Under the rotating condition, the centrifugal and Coriolis force present in the flow fields inside the turbine has changed the mixing-dilution flow field configuration of the jet flow and main stream. Compared with the flow fields in a stationary turbine cascade, the impact of rotation on the flow fields at the blade pressure side is obviously larger than that at the blade suction side. Meanwhile, an increase in air blowing ratio will expand the area of mixing-dilution flow field zone of the jet-flow and main stream and the jet-flow wake zone area. **Key words:** rotary air-cooled turbine, PIV (Particle Image Velocimeter) measurement, air blowing ratio, flow field

压气机动态模型的建立及喘振过程分析 = **Establishment of a Dynamic Model for a Compressor and Analysis of the Surge Process** [刊, 汉] / WANG Wei-cai, WANG Yin-yan (College of Power and Energy Source Engineering under Harbin Engineering University, Harbin, China, Post Code: 150001) // Journal of Engineering for Thermal Energy & Power. — 2007, 22(2). — 124 ~ 128

In environment SIMULINK, a dynamic mathematical model for a compressor has been established. To simulate the compressor surge and rotating stall phenomenon, the characteristics chart of the compressor was extended to a negative flow zone with the time delay of gas passing through the compressor being taken into consideration. The compressor surge process has been simulated and the pressure signals of the compressor have undergone a fast Fourier transformation. The compressor surge has also been tested. The simulation results show that the model can forecast the oscillation frequencies of pressure, flow rate and rotating speed as well as relevant amplitudes during the compressor surge. Structural parameters such as the rotating inertia of the compressor system and the volume of the pressure stabilizing chamber etc. may influence the surge characteristics. The model displays good dynamic regulation characteristics and can be used for a compressor control system, offering benefits of a wider-ranging practical applicability. **Key words:** compressor, dynamic model, surge, fast Fourier transformation